Title: Performance of alginate films for retention of L-(+)-ascorbic acid

Author: M.D. De'Nobili L.M. Curto J.M. Delfino M. Soria E.N. Fissore A.M. Rojas

PII: S0378-5173(13)00328-1
DOI: http://dx.doi.org/doi:10.1016/j.ijpharm.2013.04.027
Reference: IJP 13269

To appear in: *International Journal of Pharmaceutics*

Received date: 21-11-2012
Revised date: 22-2-2013
Accepted date: 7-4-2013

Please cite this article as: De'Nobili, M.D., Curto, L.M., Delfino, J.M., Soria, M., Fissore, E.N., Rojas, A.M., Performance of alginate films for retention of L-(+)-ascorbic acid, *International Journal of Pharmaceutics* (2013), http://dx.doi.org/10.1016/j.ijpharm.2013.04.027

Performance of alginate films for retention of L-(+)-ascorbic acid

M.D. De'Nobili[a], L.M. Curto[b], J.M. Delfino[b], M. Soria[c], E.N. Fissore[a], A.M. Rojas[a]*

[a]*Departamento de Industrias, Facultad de Ciencias Exactas y Naturales, University of Buenos Aires, Ciudad Universitaria, 1428 Buenos Aires, Argentina.*

[b]*Department of Biological Chemistry and Institute of Biochemistry and Biophysics – IQUIFIB (CONICET), Facultad de Farmacia y Bioquímica, University of Buenos Aires, Junín 956, 1113 Buenos Aires , Argentina . E-mail: lcurto@qb.ffyb.uba.ar*

[c]*Microbiología Agrícola, Instituto de Investigaciones en Biociencias Agrícolas y Ambientales – INBA (CONICET), Facultad de Agronomía. University of Buenos Aires, Av. San Martin 4453, 1417 Buenos Aires, Argentina. E-mail: soria@agro.uba.ar*

* Corresponding author. Tel./ fax: + 54-11-4576-3366.

***E-mail address*: arojas@di.fcen.uba.ar (A. M. Rojas)**

ABSTRACT

In view of acting as controlled delivery systems for nutritional supplementation, therapy or antioxidant activity at interfaces, alginate films of different copolymer composition and glycerol plasticizer levels were developed in the presence of Ca^{2+} for achieving higher stability of L-(+)-ascorbic acid (AA). The ability of the alginate network to preserve AA from hydrolysis, tested by storage under vacuum at 25ºC, only decreased with the relative humidity (RH) increase when alginates were mainly constituted by guluronic-guluronic acid blocks (GG), whereas also decreased with the glycerol level increase when mannuronic-mannuronic acid (MM) and/or alternating guluronic-mannuronic (GM+MG) flexible blocks were present in higher proportions. This result could be probably related to the lower capability of the latter alginate block compositions to immobilize water in the network as they are not able to constitute Ca^{2+} mediated junction zones where water molecules are highly retained. Films also studied under air storage showed that even at less favorable conditions of RH and glycerol levels, both GG or GM+MG enriched alginate networks in general preserved AA from oxidation. It also demonstrated that hydrolysis is the principal way by which AA is lost when supported in films.

***Keywords*:** alginate films, ascorbic acid hydrolysis, glycerol, biomolecule delivery, antioxidant interface.

1. Introduction

Alginate is a biomaterial that has found numerous applications in biomedical science and engineering due to its favorable properties, including biocompatibility and facility for gelation (Lee and Mooney, 2012). Alginate hydrogels have been particularly attractive in wound healing, drug delivery, and tissue engineering applications, as these gels retain structural similarity to the extracellular matrices in tissues and can be manipulated to play several critical roles. Alginates are also very useful because of their utility in preparing hydrogels at mild pH and temperature conditions, suitable for sensitive biomolecules (Pawar and Edgar, 2012). Alginic acid, a natural polysaccharide harvested from brown algae, is an unbranched binary copolymer constituted by (1,4)-linked β-D-mannuronic acid (M-block), α-L-guluronic acid (G-block) and sequences of alternating β-D-mannuronic and α-L-guluronic acid (MG-block) (Jothisaraswathi et al., 2006). Physical and mechanical properties as well as biocompatibility of alginate materials are highly dependent on the relative content of L-guluronic to D-mannuronic acids (Klöck et al., 1997; Stabler et al., 2001). Calcium ions can replace in part the hydrogen bonding, zipping guluronate (but not mannuronate) chains together stoichiometrically in an "egg-box" conformation. Guluronate chain pairing through junction zones involves three components: uronate chains, calcium ions and water molecules. The antiparallel arrangement is the macromolecular interaction probably favored in the gel, showing a notable contribution of hydrogen bonds to gel strength. Moreover, the antiparallel association of 2_1 helical chains is the arrangement found in the solid state (Braccini and Pérez, 2001).

Alginates of different monomeric composition can be assayed in their ability to form film matrices for compartmentalization of L-(+)-ascorbic acid (AA), also known as vitamin C. Through a delivery film, AA could provide, for example, nutritional

supplementation (Durschlag et al., 2007), selective killing of cancer cells or local treatment of infections where H_2O_2 (formed from AA) may be beneficial (Chen et al, 2005). AA is a water soluble reducing agent and a natural antioxidant which also can be used for pharmaceutical preservation. AA stability is affected by processing and storage conditions because it depends on a large number of factors such as temperature, equilibrium RH, oxygen partial pressure, light (Kitts, 1997). AA reacts with oxygen to produce L-dehydroascorbic acid (DHA) that also has vitamin C activity in vivo. Biological activity is irreversibly lost when DHA is hydrolyzed in the subsequent reaction. Furthermore, anaerobic degradation of AA through hydrolysis also occurs simultaneously to AA oxidation when oxygen is present, producing 2-keto-L-gulonic acid (Kurata and Sakurai, 1967). On the other hand, non enzymatic browning also proceeds with AA concentration decay since the products of the reactions that follow the first step of AA destruction are also part of the browning reaction chain (León and Rojas, 2007). Compartmentalization of AA into a film network could help achieve stabilization because it can preclude the AA interaction with oxygen, with other pharmaceutical preservatives or chemical components of the system where the film is applied, and films can constitute controlled delivery systems and provide localized antioxidant activity at interfaces. In order to evaluate the ability of alginate matrices to stabilize AA, the objective of the present work was to study the effect of alginate composition and level of glycerol (plasticizer) applied to film constitution as well as of the RH (33.3; 57.7, 75.2%) used for film storage (25ºC) on the hydrolytic and oxidative stability of AA in these matrices.

2. Materials and Methods

2.1. Chemicals

Manugel DM and Protanal LF240 alginates were a gift from FMC BioPolymer (Billingstad, Norway). Cargill (Mechelen, Belgium) and Sigma-Aldrich (herein called "VR") alginates were also used in this study. All other chemicals were of analytical grade from Merck (Argentina) or Sigma-Aldrich (St. Louis, MO, USA). Deionized water (Milli-Q, USA) was used.

2.2. Analyses of alginates

The diadic frequency composition of alginate (F_{GG}, F_{MM} and F_{GM+MG}) or block-proportions were determined by means of circular dichroism. Spectra of samples containing ≈ 0.8 mg/mL of alginate in deionized water were recorded on a Jasco J-810 (Japan) spectropolarimeter. Data in the far UV (195-250 nm) region was collected at 25ºC using a 2 mm path length cuvette. A scan speed of 20 nm/min with a time constant of 1 s was used. Each spectrum was measured four times and the data was average to minimize noise. Deconvolution of experimental spectra was done according to the procedure described by Donati et al. (2003). Mollar ellipticity was calculated using a mean residue weight value of 176.14 (the molecular weight of the monomer minus one water molecule). The diadic composition calculations were performed according to Donati et al. (2003). Based on these results the four alginates above mentioned were then selected among others for film development.

Afterwards, these four alginates were submitted to chemicals assays to determine the total acid carbohydrate content according to the spectrophotometric method of Edstrom (1969), using 4,5,4',5'-dibenzo-3,3'-diethyl-9-methylthio-carbocyanine

bromide. The protein content was determined according to Lowry et al. (1951). Methanol and acetyl contents respectively derived from methoxyl esterification of carboxylate groups and acetate ether bonding to –OH groups of the acid polysaccharides (alginates), were determined according to Wood and Siddiqui (1971) and Naumenko and Phillipov (1992), respectively. The degree of methyl esterification (DM) and acetylation (DA) of the acid polysaccharides were then calculated as:

$$DM = 100 \cdot \frac{moles_{CH_3OH}}{moles_{total\ acid\ carbohydra\ tes}}$$

$$DA = 100 \cdot \frac{moles_{CH_3COO^-}}{moles_{total\ acid\ carbohydra\ tes}}$$

Molecular weight profile of alginates was determined through gel filtration using a Fast Protein Liquid Chromatograph (FPLC, Pharmacia, Sweden) with a Superose 12HR 10/30 column (Amersham Biosciences-GE Healthcare, USA). Each alginate sample was dissolved and also eluted by using 0.5 M of imidazole buffer (pH 7.0) (Mort et al., 1991) or deionized water, at 0.5 mL/min. Dextrans of 65,000 and 40,210 molecular weights as well as blue dextran, $CoCl_2$ and sucrose were used as standards for column calibration at both elution conditions. A pectin of known molecular weight was used as reference to control the column performance under both elution conditions. Total carbohydrate content was determined into each collected fraction by the phenol-sulfuric acid spectrophotometric method (Dubois et al., 1956) when samples were collected with 0.5 M imidazole buffer (pH 7.0), and according to the method of Edstrom (1969) when samples were collected with deionized water. The former colorimetric technique underestimated the content of alginates in each fraction.

Iron and copper contents in the alginates were directly determined through inductively coupled plasma atomic emission spectrometry (ICP-AES), using a Thermo Jarrel Ash Atom Scan 25 (Thermo Jarrel, USA), according to Rubio et al. (2009).

2.3. Film formation

For the purpose of this study, each film system was developed from one of the four alginates above mentioned. A 2% (w/w) alginate concentration was used for the film making solution, thus permitting to obtain plasticized films with the adequate handling resistance. The aqueous solution was continuously stirred under controlled high speed (1,400 rpm-constant) using a vertical stirrer (LH model, Velp Scientifica, Italy) in order to reach homogeneous hydration. While stirring, the obtained viscous, homogeneous and transparent system was then heated up to 85ºC at a constant heating rate (5.3 ºC/min) by means of a hot plate (Velp Scientifica, Italy) and with simultaneous recording of the temperature by using a thermocouple connected to a Consort millivoltmeter (P901, Belgium). The following substances were subsequently added: glycerol [26.7, 35.6 or 52.3 g per 100g of (polymer+glycerol)] for plasticization (Yang and Paulson, 2000), potassium sorbate (0.030% w/w) as antimicrobial agent and AA (0.100% w/w). Finally, 1.1×10^{-3} moles of Ca^{2+} (as $CaCl_2.2\ H_2O$) were added for gelling after cooling. The hot solution was placed under vacuum for 20 s to remove air bubbles and then immediately poured onto horizontally leveled polystyrene plates. The solution dispensed into each identified plate was weighted in an analytical scale (0.0001 g-precision) in order to have constant thickness as well as a known initial content of AA into the subsequently generated film. The fractionated system was dried for 2.5 hours in a forced convection oven at 60 ºC. Films were also weighted after drying, peeled from

the polystyrene plates and stored in light-protected desiccators over saturated solutions of known water activity (a_W^o), in order to maintain a constant RH for film equilibration:

$$a_W^o = \frac{RH\%}{100}$$

The salts used were $MgCl_2$ (a_W^o = 0.333), NaBr (a_W^o = 0.577) and NaCl (a_W^o = 0.752) at 25 ºC (Greenspan, 1977). Equilibration was followed by the daily measurement of a_W in the film samples until attaining the final equilibrium. Afterwards, the sample thickness was measured at six different locations in each of ten specimens by using a digital micrometer (Mitutoyo, Kawasaki, Japan).

Three batches of films (replicates) were prepared as above described. The film samples obtained from each batch were identified and distributed among the light-protected desiccators with the different RHs (33.3; 57.7 or 75.2%) and stored at 25 ºC in order to establish the influence of the film making in the following determinations. Storage was first performed under vacuum (P = 130 Pa) with controlled RH in order to ensure that AA degradation begins through the irreversible hydrolysis of its lactone ring as the first and limiting reaction step (León and Rojas, 2007). Hence, the specific influence of water in the AA stability could be analyzed. On the other hand, samples of the three batches of Cargill and Sigma (VR) alginate films made with 35.6 or 52.3% of glycerol were further stored under normal air conditions (P = 1.013×10^5 Pa), protected from light, at 25ºC and 57.7% or 75.2% RH, in order to also infer the specific influence of oxygen on the total kinetic of AA destruction.

The following analyses were performed on each film sample collected from the three batches at each corresponding time, glycerol level and RH of interest.

2.4. Water activity

To evaluate film equilibration, the true water activity (a_Wº) was determined on the film samples with a Decagon AquaLab (Series 3 Water activity meter, USA) at 25 ºC, using a calibration curve made with the standard saturated salt solutions of $MgCl_2$, NaBr and NaCl mentioned before.

2.5. Measurement of pH

This was performed on the gel-forming solutions as well as on films equilibrated at the corresponding RH, using a bulb-combined glass electrode or a flat surface electrode (Phoenix, AZ, USA) connected to a pH meter (Consort P901, Belgium). Film pH was determined after a slight surface hydration with 20.0 µL deionized water (Joel et al., 1972). Standard buffer solutions (pH 4.00 and 7.02) were used for calibration.

2.6. Determination of L-(+)-ascorbic acid (AA)

A film sample taken from each of the three batches of films stored at each RH was carefully cut into pieces smaller than 1-mm in size, weighed on an analytical scale (0.0001 g), placed into a 25.00 ml-volumetric flask with a 1%(w/v)-oxalic acid solution and submitted to magnetic stirring for 1.5 h at 5 ºC to achieve the total extraction of AA from the film sample. During this time, it was also submitted to vortexing (Velp, Italy) for 90 s at 35 Hz, every 15 min. The suspension was finally centrifuged at 10,000 rpm and 6 ºC for 30 min (Eppendorf 5810R, USA). An aliquot was taken from the supernatant and the AA concentration was determined by using the 2,6-dichloro phenol indophenol (2,6-DPIP) spectrophotometric method (Rojas and Gerschenson, 1991) though xylene was not used for extraction of the remaining 2,6-DPIP. The AA concentration was determined in two different aliquots (duplicate) for each film sample.

The initial amount of AA into each identified film sample was known because the solution dispensed into each plate and the corresponding film obtained after drying were both weighted as indicated above. In a previous assay, the AA concentration was spectrophotometrically determined in 10 films of three different batches (n=30) which were processed as described, and it was compared with the expected concentration. The recovery of AA from the films assayed to determine the optimum experimental conditions for extraction ranges from 98.9 to 104.6%. Good interday (relative standard deviation, RSD ≤ 2.84%) and intraday (RSD ≤ 1.98%) precision was achieved.

The procedure retains its accuracy up to 81% of AA degradation kinetics. The calibration curve was constructed with nine AA concentrations ranging between 0 and 34 μg/mL every time the 2,6-DPIP solution was prepared. Regression analysis of Beer's plots showed good correlation in the 0 and 34 μg/mL concentration range, showing the same regression parameters [interception= 0.616 ± 0.001; slope= $-(725\pm3)\times10^{-5}$; residual standard error = 8.7×10^{-6}; R^2 = 0.9997]. The limit of detection of the spectrophotometric method is 0.68 μg/mL.

2.7. Color

Measurement of the film color was performed in each sample according to the ASTM E1925 (1995) employing a Minolta colorimeter (Minolta CM-508d) with an aperture of 1.5 cm-diameter (León and Rojas, 2007). Film samples for color measurement were taken from each of the three batches of films obtained in order to determine the kinetics of browning (yellowness index, YI %) increase. Also, L, a, and b (HunterLab) color parameters were measured, which ranged from L = 0 (black) to L = 100 (white or maximum) for lightness (L); $-a$ (greenness) to $+a$ (redness), and $-b$

239 (blueness) to +*b* (yellowness). Standard values considered were those of the white
240 background.
241
242 *2.8. Moisture or water content*
243 Films were sampled after equilibration at each RH, cut into pieces smaller than
244 1-mm size, weighed (0.0001 g) and placed into small, light glass containers. Samples
245 were dehydrated in a vacuum oven at 70ºC until constant weight, which involved
246 approximately 22-30 days. Determinations were performed on six film specimens at
247 each evaluated condition. Moisture or water content was informed on dry basis.
248
249 *2.9. Glass transition temperature (T_g).*
250 Modulated differential scanning calorimetry (MDSC, TA Instruments, USA)
251 was used to determine the T_g (midpoint temperature) from the second scan performed
252 on an equilibrated film sample (10–15 mg) placed into an hermetically sealed 40 μL-
253 aluminium medium pressure pan. An empty pan served as reference. Temperature was
254 brought down to −140ºC (20ºC/min) followed by a 5 min-isotherm at −140ºC. A ±
255 0.5ºC every 40 s modulation was applied. A ramp was then performed up to 40ºC
256 (10ºC/min), followed by a second decrease in temperature to −140ºC (20ºC/min), and a
257 5 min-isotherm at −140ºC. Afterwards, a second ramp was performed up to 200ºC
258 (10ºC/min), from which the T_g value was determined. MDSC was periodically
259 calibrated with a sapphire disk, in the full temperature range at which the equipment is
260 usually employed.
261
262 *2.10. Statistical analyses*

263 The results are reported as the average and standard deviation. Rate constants of
264 AA destruction (k_{AA}' and k_T) were calculated by linear regression according to a first
265 order reaction, where each experimental point corresponded to the ratio between the AA
266 concentration remaining at a given storage time t (C_{AA}) and the initial (t = 0)
267 concentration of AA (C_{AA}^{o}):

268 $$C_{AA}(t) = \frac{weight_{AA}(t)}{weight_{film}}$$

269 wherein the "weight" is expressed in grams.

270 Browning rate constants (k_{YI}) were calculated from the slope of the linear
271 regression of experimental data (YI% *vs* time). Analysis of covariance (ANCOVA) was
272 applied for comparison of slopes, that is, of the rate constants (k_{AA}' and k_T, or k_{YI}), as
273 indicated by Sokal and Rohlf (2000). The statistical analyses of results were performed
274 by applying ANOVA (α: 0.05), followed by pairwise multiple comparisons evaluated
275 by Tukey's significant difference test. The GraphPad Prism software (version 5.00,
276 2007, GraphPad Software Inc., USA) was used for all analyses previously detailed.

277 The effect of two quantitative factors (RH and glycerol) on the calculated rate
278 constants (k_{AA}' and k_{YI}) were analyzed with a complete 3×3 experimental design at the
279 three levels described before for both factors, coded as −1, 0, +1. This design was
280 repeated for the four polymer tested. In the first model the polymer type was included as
281 a categorical variable, but subsequently each polymer was analyzed separately. A
282 regression model was applied as a function of the lineal and quadratic values of the
283 quantitative factors and their interactions. This statistical analysis was performed with R
284 (version 2.15: R Core Team, 2012).

285

286 **3. Results and Discussion**

287

288 *3.1. Polymer characterization*

289 The relevant molecular characteristics of the alginate polymers used in this work
290 are listed in **Table 1**. Proteins were not detectable. Alginates showed an acidic
291 polysaccharide content of ≈ 95% (Edstrom, 1969) and they were no methoxyl-esterified.
292 As expected from algal alginates, O-acetyl groups were absent (Davidson et al., 1977).
293 Similar and low amounts of iron and copper were observed (**Table 1**). Molecular
294 weights and their distributions were similar (≈ 876 kDa). This value corresponds to a
295 high molecular weight alginate which is reported to be related to higher viscosity
296 (Aoyama et al., 2007). Important biophysical properties of alginates are also related to
297 the molecular weight (Kong et al., 2004).

298 The high selectivity of alginate binding towards calcium ions, which accounts
299 for its capacity to form ionotropic gels, is determined by the polymer composition
300 (Simpson et al., 2004). Furthermore, parameters such as the stability, strength and
301 porosity of the obtained gels are influenced by the diadic frequency composition (F_{GG},
302 F_{GM+MG} and F_{MM}) of alginate (Donati et al., 2003). In order to study the influence of the
303 macromolecule structure in the development of film networks able to stabilize AA,
304 alginates with different monomeric composition were then used in this work. Alginate
305 composition and block-proportions can be determined by the circular dichroism
306 characteristics of alginate molecules (Morris et al., 1980; Klöck et al., 1997; Donati et
307 al., 2003). Circular dichroism spectra are shown in **Fig. 1**. All polymers used showed
308 the negative MG and GG diads bands. The circular dichroism spectra of Manugel and
309 Cargill alginates were characterized by the minima at 210 nm (≈ −1330 and −1260
310 molar ellipticity, respectively), whereas VR and Protanal alginates show a shallower
311 spectra with minima at 213 nm (≈ −1050 for both alginates). These features can account

312 for the different diadic composition. According to the procedure described by Donati et
313 al. (2003), deconvolution of experimental spectra (**Fig. 1**) allowed calculating the diadic
314 composition (F_{GG}, F_{MM} and F_{GM+MG}), and results are shown in **Table 1**. Manugel
315 alginate was mainly constituted by GG-blocks, with lower proportion of MM-blocks.
316 Cargill alginate showed lower proportion of GG- and MM-blocks than Manugel
317 alginate, but Cargill differs mainly in its higher proportion of flexible GM+MG-blocks.
318 On the other hand, Protanal and VR alginates showed similar composition, although
319 Protanal was characterized by a higher proportion of MM-blocks and a lower one of
320 GM+MG-blocks.

321 Contrary to polymannuronates, a high affinity of polyguluronates to calcium
322 ions was determined by Kohn (1975). By studying the encapsulation of βTC3 cells,
323 Simpson et al. (2004) determined that alginate with high mannuronic acid content was
324 not affected by changes in $CaCl_2$ concentration due to the low percentage of consecutive
325 guluronic acid residues. A cooperative effect in calcium binding is observed for
326 polyguluronic acid at chain lengths above a threshold of ≈ 20 residues (Braccini and
327 Pérez, 2001; Fang et al., 2008). The alginate fragments with alternating sequence of D-
328 mannuronic and L-guluronic acid units (GM+MG-blocks) exert only a low selectivity in
329 ion exchange reaction, whereas the affinity of the monomers (D-mannuronate, L-
330 guluronate) to calcium ions was found to be virtually the same (Kohn, 1975). GG-
331 blocks are the most inflexible ones in alginate macromolecules, whereas GM+MG-
332 blocks are the most flexible. Chain breakage by oxidants was demonstrated to occur
333 mainly at the most flexible blocks of the alginate macromolecules, whereas the GG-
334 block length largely determines the elastic modulus of calcium cross-linked gels (Kong
335 et al., 2004). In the present work, the amount of Ca^{2+} required for gelling of the film
336 making solutions was then calculated from the proportion of GG-blocks, being it

reported in **Table 1**. For film formulations, 1.1×10^{-3} moles of Ca^{2+} were then used in order to satisfy a minimum requirement for all alginates. This content also permits to obtain films with an adequate handling flexibility, especially at the lowest level of glycerol used for plasticization.

3.2. Film characteristics

Homogeneous and flexible films plasticized by glycerol proportions of 26.7, 35.6 or 52.3%w/w were obtained after casting from each alginate solution. Films were transparent, almost colorless or yellowish (b = +6 to +9; YI = 12-18%) and showed high initial lightness (**Table 2**). The AA concentration initially determined (C_{AA}^{o}) was ≈ 3.02×10^{-2} g AA per g of film, which means that a 100% of AA recovery was achieved after casting. Temperature should be as low as possible to get short periods of drying (≤ 2.5 hours), which avoid AA losses through hydrolysis during this processing. Therefore, films were finally dried at 60ºC. Film samples attained equilibration at 20 hours of vacuum storage at each RH, as determined by measurement of the film a_W^{o} (0.333, 0.577 and 0.752, respectively) at 25ºC. Thickness measured after equilibration was ≈ 0.12 mm (**Table 2**). There was not significant influence of RH and glycerol content on film thickness. The film pH recorded along storage varied as indicated in **Table 2**. Moisture contents increased with the RH of film equilibration. In general, the increase in the glycerol level produced a significant increase in the moisture content only for films equilibrated at 75.2% RH (**Table 3**).

At ≈ –38ºC and/or 0ºC, MDSC scans did not show any endothermic peak that could correspond to freezable bound and free water, respectively (Hatakeyama and Hatakeyama, 1998). Therefore, water gained from the storage environment was

adsorbed or retained by the polymeric network. The T_g values found for all equilibrated films herein studied were lower than the storage temperature (25ºC) (**Table 3**). Hence, the equilibrated films were amorphous rubber materials at ambient temperature. Into each type of alginate assayed, T_g values in general decreased significantly ($p < 0.05$) with the increase in the glycerol proportion used as well as in the water content (**Table 3**). Hence, glycerol as well as the water captured during storage plasticized the film networks. At each level of glycerol, Manugel alginate films showed, in general, the highest values of T_g and, hence, the lowest macromolecular mobility. Probably, this result may be associated with its higher proportion of inflexible GG-blocks and/or with a very small proportion of flexible GM+MG-blocks (**Table 1**). According to Roger et al. (2004), powder samples of alginate exhibited T_g ranging from 95°C to 136°C and no significant effect on T_g was observed for different molecular weight samples. However, an increase in T_g values with the G content was observed. This effect was attributed to the presence of residual Ca^{2+} ions in the alginate powder, crosslinking oligomeric G-rich chains.

Alginates are block copolymers and, hence, they can behave as two-phase systems or physical blends. Each phase exhibits its own distinct T_g (Ferry, 1980). Only one T_g was detected in thermograms of alginate films developed in the present work. This could be attributable to a plasticization effect and/or to a probable random alternating distribution of blocks in the alginate macromolecules.

3.3. Stability of L-(+)-Ascorbic Acid to Chemical Hydrolysis in Films

The study of AA stability by storage in the absence of air (P = 130 Pa) allowed to determine that the ratio between the remaining AA concentration [$C_{AA}(t)$] and the

387 initial one [C_{AAO}] statistically changed with the storage time (t) according to a pseudo-
388 first order ($p < 0.05$) kinetic law (Leon and Rojas, 2007). The rate constants of AA
389 hydrolysis (k_{AA}') were then calculated from the slope obtained after fitting a straight
390 line to the data. On the other hand, browning development was measured as the
391 increment of the YI with time, which statistically fitted ($p < 0.05$) to a pseudo-zero
392 order reaction (Rojas and Gerschenson, 2001). Browning rate constant (k_{YI}) was then
393 calculated from each slope obtained after linear regression fitting to the experimental
394 data. The AA stability to hydrolysis (k_{AA}' values) seemed to be mainly affected by the
395 glycerol level as well as by the RH of film storage at 25ºC, as shown in the example
396 depicted in **Fig. 2**. Similar conclusions were drawn from comparison of k_{YI} values.

397 Collected k_{AA}' data was analyzed by an experimental design of two quantitative
398 factors (RH and glycerol) at the three levels described before, coded as –1, 0, +1. A
399 regression model was applied to analyze k_{AA}' as a function of the linear and quadratic
400 values of the quantitative terms and their interactions. In a preliminary analysis, the type
401 of polymer was considered as a third quantitative factor which differed in the frequency
402 composition of each alginate (F_{GG}, F_{MM} and F_{GM+MG}) applied to film development. It
403 was observed that AA hydrolysis was only affected by a significant interaction between
404 Protanal ($p < 0.001$) or VR ($p < 0.05$) and the alginate diadic composition and glycerol
405 levels. Hence, only RH and glycerol were considered finally as quantitative factors and
406 separated models were built for each type of polymer.

407 The statistical results are reported in **Table 4**. The experimental design of RH
408 and glycerol factors indicated that the rate constant of AA hydrolysis (k_{AA}')
409 significantly ($p < 0.05$) increased as a consequence of the separated increase in RH or
410 glycerol content, when AA was compartmentalized in Protanal or VR alginate
411 networks. It has been suggested that the previous presence of glycerol permits or

412 facilitates the penetration of water into the polymeric network during storage (Pérez et
413 al., 2009). On the other hand, k_{AA}' only increased significantly ($p < 0.05$) with the RH
414 of film storage when AA was supported either in Manugel ($p < 0.05$) or Cargill ($p <$
415 0.001) alginate network. The dependence was also significant ($p < 0.05$) for the
416 quadratic term of the RH factor for Cargill alginate films. The proportion of glycerol
417 used for plasticization did not affect the AA stability in Manugel or Cargill alginate
418 film. The highest proportion of GG-block in Manugel followed by Cargill alginate
419 produces ordered templates for polymer chain associations mediated by Ca^{2+}
420 crosslinking between neighboring macromolecules (Braccini and Pérez, 2001).
421 Chandrasekaran et al. (1988) indicated that glycerol can produce disturbance of filament
422 aggregation in the case of gellan polymer, which may also be extended to Manugel and
423 Cargill alginate films. However, zipping of GG-block chains together by calcium ions
424 may overcome the glycerol effect in these films. As previously mentioned, GG-block
425 length determines the elastic modulus of calcium cross-linked alginate gels (Kong et al.,
426 2004).

427 A somewhat higher hydrolytic stability of AA supported in Manugel or Cargill
428 alginate films is observed by plotting the rate constants of AA hydrolysis (k_{AA}') *versus*
429 glycerol or RH linear factor (**Fig. 3**), especially by storage at 33.3% of RH but also at
430 75.2%. Hence, alginates with a predominant proportion of GG-blocks showed a higher
431 ability to stabilize AA against hydrolysis. This effect could be associated with their
432 higher capability to immobilize water by physical retention, as previously demonstrated
433 for gellan films (León and Rojas, 2007). As mentioned above, guluronate chain pairing
434 junction zones also involve water molecules (Braccini and Pérez, 2001), which
435 correspond to highly adsorbed or non-freezable bound water (Ping et al., 2001).

436 Water is responsible for hydrolysis and the irreversible opening of the lactone
437 ring of the AA molecule, producing 2-keto-L-gulonic acid (Kurata and Sakurai, 1967).
438 Hence, at constant temperature (25ºC), k_{AA}' depended on the RH factor because k_{AA}' is
439 the product of the true second order rate constant for AA hydrolysis (k) and the
440 concentration of water available for reactions (C_{WATER}) (León and Rojas, 2007). This
441 kind of water is that loosely retained by the solid-like film network. As RH of film
442 equilibration increases, the polymeric network leaves higher proportion of loosely
443 adsorbed water, which is available for chemical reactions. This condition also promotes
444 the parallel development of browning reactions from 2-keto-L-gulonic acid.

445 The half-life times ($t_{1/2}$) of the AA supported in the alginate films were
446 calculated from the values for k_{AA}'. In the most favorable condition of RH (33.3%), $t_{1/2}$
447 values ranged between 10 and 16 months for AA supported in Manugel and Cargill
448 alginate films, a result not affected by the glycerol level, and between 3 and 11 months
449 in Protanal and VR alginates, for decreasing proportions of glycerol. At 57.7% RH, the
450 values of $t_{1/2}$ were in general no lower than 2 months. At 75.2% RH, the AA supported
451 in Manugel alginate films showed a $t_{1/2} \approx 27$ days for all glycerol levels, whereas in VR
452 and Protanal films, the $t_{1/2}$ decreased from 32 to 14 and from 32 to 9 days, respectively,
453 as glycerol level increased.

454 The rate constants of browning development (k_{YI}) were also analyzed through
455 the experimental design applied to AA degradation kinetics, with the polymer type as a
456 categorical variable. The results indicated that k_{YI} significantly ($p < 0.01$) increased in a
457 linear trend with the RH of film storage and glycerol proportion for all polymers
458 assayed (**Table 4**), excepting for VR alginate films. In the latter system, browning
459 kinetic was only dependent ($p < 0.01$) on the RH of storage. Significant dependence of
460 k_{YI} on the RH in Cargill ($p < 0.01$) and Protanal ($p < 0.05$) alginate films was also

461 observed in a quadratic term. An interaction between RH and glycerol was also detected
462 for Protanal films. Response surfaces were then plotted (**Fig. 4**). They allowed us to find
463 the best conditions for minimal browning, which corresponded to a 41-44 % RH for
464 storage and 29% w/w of glycerol content for plasticization, whereas the highest values
465 of k_{YI} were observed at the highest RH of storage and glycerol content in films (**Fig. 4**).
466 By plotting the rate constants of browning (k_{YI}) *versus* glycerol or RH lineal
467 factor (**Fig. 3**), no clear tendencies towards slower browning were observed in film
468 systems. In general, lower k_{YI} values were obtained for Manugel alginate films at
469 increasing RH and glycerol levels.
470 Despite the different kinetic order, k_{YI} correlated significantly (Pearson's
471 correlation coefficient $r = 0.8731$; $p < 0.001$) with the k_{AA}' values.
472
473 *3.4. Stability of L-(+)-Ascorbic Acid to Chemical Hydrolysis and Oxygen in Films*
474 Films respectively made with Cargill or VR alginate using the two highest
475 glycerol proportions were also studied in their ability to stabilize AA in the presence of
476 oxygen. Storage was performed at 57.7 or 75.2% RH (25ºC) under normal air pressure
477 ($P=1.013\times10^5$ Pa). Hence, the oxygen partial pressure (p_i) was 0.21 atm constant during
478 storage. Under these conditions, a pseudo-first order kinetics could be fitted to the
479 experimental data of AA concentration ($p < 0.05$) in a manner similar to that previously
480 observed in Fig. 2 for AA loss in alginate films stored under vacuum. AA destruction in
481 the presence of oxygen occurred simultaneously to the hydrolytic reaction previously
482 studied under vacuum storage of films (Kurata and Sakurai, 1967). It can be then
483 considered that at least two irreversible parallel or competitive reactions proceed: the
484 AA hydrolysis (k_{AA}') and the AA oxidation (k_{AA}^{OX}), which can be expressed as a

485 differential kinetic equation written for the AA as the reagent, in the form of pseudo-
486 first-order rate reactions:

487 $$r_{AA} = -\frac{1}{\nu_{AA}}\frac{dC_{AA}}{dt} = k'_{AA}\cdot C_{AA}(t) + k_{AA}^{OX}\cdot C_{AA}(t) \qquad (1)$$

488 wherein ν_{AA} is the stoichiometric coefficient for AA hydrolytic reaction, r_{AA} is the AA-
489 reaction rate/unit volume at a constant temperature, $C_{AA}(t)$ is the AA concentration
490 remaining at time t, k_{AA}' is the rate constant of the pseudo first order kinetics for AA
491 hydrolysis, k_{AA}^{OX} is the oxidation rate constant of AA.

492 By integration ($\nu_{AA} = 1$), results:

493 $$C_{AA} = C_{AA}^{O}.\exp[-(k'_{AA} + k_{AA}^{OX}).t]$$

494 Hence, the slope calculated from the experimental data obtained after storage under air
495 give the total rate constant (k_T):

496 $$k_T = k'_{AA} + k_{AA}^{OX} \qquad (2)$$

497 and the oxidation rate constant (k_{AA}^{OX}) can be obtained as the arithmetic difference. For
498 oxygen partial pressures lower than 0.40 atm, the apparent rate constant (k_{AA}^{OX}; eq. 1
499 and 2) involved the product between the true kinetic rate constant of oxidation (only
500 dependent on temperature) and the oxygen concentration, related to the p_i (Khan and
501 Martell, 1967).

502 In general, film systems stored under air did not show significant differences
503 between k_T and k_{AA}' values (**Table 5**). Higher k_T values were only observed for Cargill
504 alginate film formulated with 35.6% glycerol and stored at 57.7 or 75.2% RH. Even in
505 film systems where a non significant difference between k_T and k_{AA}' was observed,
506 browning rate constants (k_{YI}) determined under air storage at 75.2% RH were in general
507 higher than the k_{YI} values found under vacuum (**Table 5**). It can be concluded that, in
508 general, the alginate film networks seemed to effectively preserve AA from oxidation.

4. Conclusions

Water is the factor responsible for AA hydrolysis, and glycerol may facilitate water penetration from the environment into the polymeric network. In the presence of Ca^{2+}, alginates with higher proportion of GG-blocks (F_{GG} = 0.66) and lower one of MM- and, mainly, of GM+MG flexible blocks, generate film networks that immobilize water sufficiently to reduce the degradation of hydro-sensitive biomolecules such as AA. When comparing the hydrolytic with the total rate constant of AA destruction under air, it was observed that even at less favorable conditions of RH and glycerol levels, both GG and GM+MG enriched alginate networks in general preserve AA from oxidation. It also demonstrated that hydrolysis is the principal way by which AA is lost when supported in films and, hence, water immobilization is a key factor to be controlled.

ACKNOWLEDGEMENTS

We greatly acknowledge FMC BioPolymer (Billingstad, Norway) and especially Dr Trond Helgerud for sending us different types of alginates. This work was supported by grants from University of Buenos Aires, National Research Council (CONICET) and Agencia Nacional de Promoción Científica y Tecnológica de Argentina (ANPCyT).

References

Aoyama, N., Hayakawa, I., Akiba, N., Minakuchi, S., 2007. Effect of high-molecular-weight sodium alginate on the viscosity and characteristics of alginate impression materials. Prosthodont Res. Pract. 6, 239-245.

534 ASTM D1925 (1995). Standard Test Method for yellowness index of plastics,.American
535 Society for Testing and Materials, Philadelphia.
536
537 Braccini, I., Pérez, S., 2001. Molecular basis of Ca^{2+}-induced gelation in alginates and
538 pectins: the egg-box model revisited. Biomacromol. 2, 1089-1096.
539
540 Chandrasekaran, R., Puigjaner, L.C., Joyce, K.L., Arnott, S., 1988. Cation interactions
541 in gellan: an X-ray study of the potassium salt. Carbohyd. Res. 181, 23–40.
542
543 Chen, Q., Graham Espey, M., Krishna, M.C., Mitchell, J.B., Corpe, C.P., Buettner,
544 G.R., Shacter, E., Levine, M., 2005. Pharmacologic ascorbic acid concentrations
545 selectively kill cancer cells: Action as a pro-drug to deliver hydrogen peroxide to
546 tissues. PNAS 102(38), 13604-13609.
547
548 Davidson, I.W., Sutherland, I.W., Lawson, C.J., 1977. Localization of O-Acetyl Groups
549 of Bacterial Alginate. J. General Microb. 98, 603-606.
550
551 Donati, I., Gamini, A., Skjåk-Bræk, G., Vetere, A., Campa, C., Coslovi, A., Paoletti, S.,
552 2003. Determination of the diadic composition of alginate by means of circular
553 dichroism: a fast and accurate improved method. Carbohyd. Res. 338, 1139–1142.
554
555 Dubois, M., Gilles, K.A., Hamilton, J.K., Robers, P.A., Smith, F., 1956. Colorimetric
556 method for determination of sugars and related substances. Anal. Chem. 28, 350–
557 356.
558

559 Durschlag, M.E., Charlotte, N.C., Kehoe, G.S., Glendale, A.Z., 2007. Edible film for
560 transmucosal delivery of nutritional supplements. United States Patent Application
561 Publication, Pub. No. US 2007/0087036 A1, Pub. date Apr. 19.
562
563 Edstrom, R.D., 1969. A calorimetric method for the determination of
564 mucopolysaccharides and other acidic polymers. Analyt. Biochem. 29, 421-432.
565
566 Fang, Y., Al-Assaf, S., Phillips, G.O., Nishinari, K., Funami, T., Williams, P.A., 2008.
567 Binding behavior of calcium to polyuronates: Comparison of pectin with alginate.
568 Carbohyd. Polym. 72, 334–341.
569
570 Ferry, J.D., 1980. Viscoelastic properties of polymers, third ed. John Wiley & Sons,
571 New York.
572
573 Greenspan, L., 1977. Humidity fixed points of binary saturated aqueous solutions. J.
574 Res. Nat. Bur. Stand. 81 A(1), 89-96.
575
576 Hatakeyama, H., Hatakeyama, T., 1998. Interaction between water and hydrophilic
577 polymers. Therm. Acta 308, 3-22.
578
579 Joel, A., Indictor, N., Hanlan, J.F., Baer, N.S., 1972. The measurement and significance
580 of pH in paper conservation. Bulletin of the American Group. Int. Inst. Conserv. Hist.
581 Art. Works 12(2), 119-125.
582
583 Jothisaraswathi, S., Babu, B., Rengasamy, R., 2006. Seasonal studies on alginate and its
584 composition II: Turbinaria conoides (J.Ag.) Kütz. (Fucales, Phaeophyceae). J. Appl.
585 Phycol. 18, 161–166.

Khan, M.M.T., Martell, A.E., 1967. Metal ion and metal chelate catalyzed oxidation of ascorbic acid by mo1ecuIa.r oxygen. 1. Cupric and ferric ion catalyzed oxidation. J. Am. Chem. Soc. 89, 4167-4179.

Kitts, D.D., 1997. An evaluation of the multiple effects of the antioxidant vitamins. Trends Food Sci. Techn. 8, 198-203.

Klöck, G., Pfefferrnann, A., Ryser, C., Gröhn, P., Kuttler, B., Hahn, H.J., Zimmermann, U., 1997. Biocompatibility of mannuronic acid-rich alginates. Biomater. 18, 707-713.

Kohn, R., 1975. Ion binding on polyuronates. Alginate and pectin. Pure Appl. Chem. 42, 371-397.

Kong, H.J., Kaigler, D., Kim, K., Mooney, D.J., 2004. Controlling rigidity and degradation of alginate hydrogels via molecular weight distribution. Biomacrom. 5, 1720-1727.

Kurata, T., Sakurai, Y., 1967. Degradation of L-ascorbic acid and mechanism of nonenzymic browning reaction. Part I. Agric. Biol. Chem. 31, 101-105.

Lee, K.Y., Mooney, D.J., 2012. Alginate: Properties and biomedical applications. Prog. Polym. Sci. 37, 106-126.

León, P.G., Rojas, A.M., 2007. Gellan gum films as carriers of L-(+)-ascorbic acid. Food Res. Int. 40, 565-575.

Lowry, O.H., Rosebrough, N.J., Farr, A.L., Randall, R.J., 1951. Protein measurement with the Folin phenol reagent. J. Biol. Chem. 193, 265–275.

Morris, E.R., Rees, D.A., Thom, D., 1980. Characterization of alginate composition and block-structure by circular dichroism. Carbohyd. Res. 81, 305-314.

Mort, A.J., Moerschbacher, B.M., Pierce, M.L., Maness, N.O., 1991. Problems encountered during the extraction, purification, and chromatography of pectic fragments, and some solutions to them. Carbohyd. Res. 215, 219–227.

Naumenko, I.V., Phillipov, M.P., 1992. Colorimetric method for determination of acetyl groups in pectic substances. Akad. Nauk Repub. Moldova Biol. Khim. Nauk. 1, 56-59 (in Russian).

Pawar, S.N., Edgar, K.J., 2012. Alginate derivatization: a review of chemistry, properties and applications. Biomat. 33, 3279-3305.

Pérez, C.D., Flores, S.K., Marangoni, A.G., Gerschenson, L.N., Rojas, A.M., 2009. Development of a high methoxyl-pectin edible film for retention of l-(+)-ascorbic acid. J. Agric. Food Chem. 57, 6844-6855.

Ping, Z.H., Nguyen, Q.T., Chen, S.M., Zhou, J.Q., Ding, Y.D., 2001. States of water in different hydrophilic polymers-DSC and FTIR studies. Polym. 42, 8461-8467.

R Core Team, 2012. R: A language and environment for statistical computing. R Foundation for Statistical Computing, Vienna, Austria. ISBN 3-900051-07-0, URL http://www.R-project.org/

Roger, S., Bee, A., Balnois, E., Bourmaud, A., Le Deit, H., Grohens, Y., Cabuil, V., 2004. Physical and mechanical properties of alginate films containing calcium cations

644 and ferrofluids. Fifth International Conference Polymer-Solvent Complexes &
645 Intercalates. July 11-14, Lorient, France.
646
647 Rojas, A.M., Gerschenson, L.N., 1991. Determinación de vitamina C en productos
648 frutihortícolas. An. Asoc. Quím. Arg. 79(2), 97-106.
649
650 Rojas, A.M., Gerschenson, L.N., 2001. Ascorbic acid destruction in aqueous model
651 systems: an additional discussion. J. Sci. Food Agric. 81(15), 1433-1439.
652
653 Rubio, C., Gutiérrez, A.J., Revert, C., Reguera, J.I., Burgos, A., Hardisson, A., 2009.
654 Daily dietary intake of iron, copper, zinc and manganese in a Spanish population.
655 International J. Food Sci. Nutr. 60(7), 590–600.
656
657 Simpson, N.E., Stabler, C.L., Simpson, C.P., Sambanis, A., Constantinidis, I, 2004. The
658 role of the $CaCl_2$–guluronic acid interaction on alginate encapsulated βTC3 cells.
659 Biomat. 25, 2603-2610.
660
661 Sokal, R.R., Rohlf, J.B., 2000. Biometry: The Principles and Practice of Statistics in
662 Biological Research, W.H. Freeman and Company, San Francisco, pp. 253-380.
663
664 Stabler, C., Wilks, K., Sambanis, A., Constantinidis, I., 2001. The effects of alginate
665 composition on encapsulated βTC3 cells. Biomat. 22, 1301-1310.
666
667 Wood, P.J., Siddiqui, I.R., 1971. Determination of methanol and its application for
668 measurement of pectin ester content and pectin methyl esterase activity. Anal.
669 Biochem. 39, 418–428.
670

671 Yang, L., Paulson, A.T., 2000. Mechanical and water vapour barrier properties of edible
672 gellan films. Food Res. Int. 33, 563-570.

673

674

674 **Figure captions**

675

676 **Fig. 1.** Circular dichroism spectra recorded for (— black) Protanal, (— thick orange
677 line) VR, (— blue) Cargill and (— red) Manugel alginates.

678

679 **Fig. 2.** Kinetics of AA hydrolysis determined in Cargill alginate films are shown for
680 two levels of glycerol and three levels of storage relative humidity (RH).

681

682 **Fig. 3.** Rate constants of AA hydrolysis (k_{AA}**'**) are plotted against glycerol (glyc.n) (**A**)
683 or relative humidity (RH.n) (**B**) linear factor. Idem for the rate constants of browning
684 development (k_{YI}): (glyc.n) (**C**) and (RH.n) (**D**).

685

686 **Fig. 4.** Relative humidity (RH) and glycerol content influences on the rate constant of
687 browning development (k_{YI}) are plotted as response surfaces for Protanal (**A**) and
688 Cargill (**B**) alginate films.

689

690

690 **Table 1**

691 Chemical composition of the alginate polymers used for film development.

692

	Alginate			
	Manugel	Cargill	VR	Protanal
Molecular weight [a] (kDa)	876 ± 180	876 ± 200	876 ± 140	876 ± 180
Protein content [a] (g / 100 g) [f]	0.10 ± 0.09	0.59 ± 0.08	0.5 ± 0.3	0.03 ± 0.06
Total acid carbohydrates [a] (g / 100 g) [f]	95.9 ± 0.8	93.0 ± 0.6	97.05 ± 0.07	95.6 ± 0.4
DM[b] (%)	0.10	0.10	0.08	0.5
DA[c] (%)	ND	ND	ND	ND
Iron [a] (mg/1000 g) [f]	45 ± 4	39 ± 6	34± 6	36 ± 5
Copper [a] (mg/1000 g) [f]	38 ± 7	42 ± 8	24 ± 7	29 ± 5
F_{GG} [d]	0.66	0.57	0.27	0.25
F_{MM} [d]	0.26	0.22	0.32	0.42
F_{GM+MG} [d]	0.08	0.21	0.40	0.33
F_G [d]	0.70	0.67	0.47	0.42
F_M [d]	0.30	0.33	0.53	0.58
Ca^{2+} required [e] (mol/100 g) [f]	2.85×10^{-3}	2.45×10^{-3}	1.18×10^{-3}	1.08×10^{-3}

693 [a] Mean and standard deviation (n = 3) are shown.
694 [b] Degree of methyl esterification is expressed as 100 × moles of methoxyl group / moles of total acid
695 carbohydrates.
696 [c] Degree of acetylation is expressed as 100 × moles of acetyl group / moles of total acid carbohydrates.
697 [d] Diadic frequency composition of GG-, MM- and GM+MG-blocks [guluronic (G); mannuronic (M)] in
698 alginates determined through circular dichroism (Donati et al., 2003). F_G and F_M are the total proportions
699 of G and M monomers, respectively.
700 [e] moles of Ca^{2+} required per 100 g of film making solution calculated from the respective F_{GG} value.
701 [f] Expressed per 100 g or 1000 g of alginate.
702 ND: non detectable.
703

703 **Table 2**

704 Color parameters[a,b] and thickness[c,d] are reported as well as the pH[a] variation recorded
705 during the complete period of film storage,.

706

Alginate	YI %	*L* %	+ *b*	Thickness (mm)	pH
Manugel	17 ± 1	82 ± 1	7.9 ± 0.3	0.100± 0.040	4.42 ± 0.07
Cargill	12 ± 2	85 ± 1	6.3 ± 0.5	0.100 ± 0.030	4.54 ± 0.08
VR	16 ± 2	80 ± 1	6.1 ± 0.6	0.140 ± 0.070	4.37 ± 0.03
Protanal	18 ± 3	80 ± 3	9 ± 1	0.110± 0.030	4.61 ± 0.03

707 [a] Mean and standard deviation ($n \geq 27$) are shown.
708 [b] Yellowness index (YI), lightness (*L*) and *b* (blue–yellow component) recorded initially.
709 [c] Mean and standard deviation ($n \geq 11$) are shown.
710 [d] It was measured after film equilibration at each relative humidity (HR) and 25ºC.
711
712
713
714

715

715 **Table 3**

716 Moisture content and glass transition temperature (T_g) determined after film
717 equilibration at each relative humidity (RH) of storage (25ºC).

Alginate	Glycerol (% w/w)	RH (%)	Moisture content[a] (g water / g *dm*)	T_g [b] (C)
Manugel	26.7	33.3	14.3 ± 0.9	–40.06
		57.7	22.9 ± 0.1	–44.18
		75.2	27.1 ± 0.1	–66.83
Cargill	26.7	33.3	17 ± 2	–59.05
		57.7	23.42 ± 0.09	–62.57
		75.2	29.8 ± 0.1	–64.37
VR	26.7	33.3	15.3 ± 0.4	–61.70
		57.7	21.4 ± 0.1	–70.57
		75.2	31.3 ± 0.4	–72.66
Protanal	26.7	33.3	17 ± 2	–63.82
		57.7	22.8 ± 0.7	–71.36
		75.2	27.9 ± 0.1	–72.46
Manugel	35.6	33.3	16.3 ± 0.2	–53.14
		57.7	23.9 ± 0.4	–65.72
		75.2	34.1 ± 0.4	–71.4
Cargill	35.6	33.3	16.0 ± 0.4	–58.00
		57.7	23.9 ± 0.4	–66.36
		75.2	28.77 ± 0.07	–72.95
VR	35.6	33.3	17.1 ± 0.5	–63.50
		57.7	23.7 ± 0.3	–71.83
		75.2	37.9 ± 0.4	–75.11
Protanal	35.6	33.3	15.8 ± 0.4	–63.81
		57.7	23.5 ± 0.9	–73.92
		75.2	33.1 ± 0.1	–75.66
Manugel	52.3	33.3	17 ± 1	–63.37
		57.7	25.1 ± 0.3	–75.21
		75.2	35.9 ± 0.6	–84.14
Cargill	52.3	33.3	16.3 ± 0.7	–68.05
		57.7	24.71 ± 0.08	–75.21
		75.2	35.7 ± 0.3	–84.53
VR	52.3	33.3	16.8 ± 0.4	–73.62
		57.7	25.5 ± 0.7	–77.00
		75.2	38.3 ± 0.2	–89.71
Protanal	52.3	33.3	17.1 ± 0.2	–74.19
		57.7	24.2 ± 0.2	–76.25
		75.2	39 ± 3	–88.43

718 [a]Mean and standard deviation (n =6) are shown.
719 [b]Mean is shown. SD is not reported because it is lower than 1% of the T_g value.
720 *dm*: dry mass.
721

Table 4

Results of the statistical analysis are summarized for the rate constants of AA hydrolysis (k_{AA}') and subsequent browning development (k_{YI}).

	Alginate			
	Manugel	Cargill	VR	Protanal
	k_{AA}'			
RH.n	**0.00148**	**0.000516**	**0.00791**	**0.0104**
RH.n^2	0.46283	**0.012284**	0.23020	0.0726
glyc.n	0.13367	0.763096	**0.04400**	**0.0227**
glyc.n^2	0.12316	0.098638	0.63613	0.3497
RH.n:glyc.n[a]	0.28204	0.209220	0.10240	0.1099
Residual standard error	1.655×10^{-6}	1.534×10^{-6}	3.583×10^{-6}	5.72×10^{-6}
Multiple R^2	0.9789	0.9901	0.9520	0.9563
F-test probability	0.0102	0.003335	0.03419	0.02985
	k_{YI}			
RH.n	**0.000963**	**0.0013**	**0.00727**	**0.000153**
RH.n^2	0.262219	**0.0071**	0.22641	**0.003147**
glyc.n	**0.016522**	**0.0343**	0.43724	**0.005224**
glyc.n^2	0.511434	0.7844	0.69191	0.474943
RH.n:glyc.n	0.074762	0.0852	0.49912	**0.011385**
Residual standard error	4.49×10^{-5}	3.142×10^{-5}	1.158×10^{-4}	4.195×10^{-5}
Multiple R^2	0.9856	0.9981	0.9396	0.9960
F-test probability	0.005814	0.004774	0.04773	0.000849

[a] In no case was the interaction between RH and glycerol level significant ($p < 0.05$) for AA hydrolytic rate constants.

Relative humidity (RH) or glycerol (glyc) linear (RH·n; glyc·n) and quadratic (RH·n^2; glyc·n^2) factors.

Bold numbers highlight significance ($p < 0.05$).

729 **Table 5**

730 Rate constants[a] of AA hydrolysis (k_{AA}') or hydrolysis and oxidation (k_T)[b], as well as of

731 browning development (k_{YI}) at 25ºC, are reported.

732

Alginate	Glycerol (% w/w)	Relative humidity (%)	*Storage without air*		*Storage under air*	
			k_{AA}' $\times 10^5$ (min^{-1})	$k_{YI} \times 10^4$ ($YI\% \cdot min^{-1}$)	$k_T \times 10^5$ (min^{-1})	$k_{YI} \times 10^4$ ($YI\% \cdot min^{-1}$)
Cargill	35.6	57.7	0.32 ± 0.01	2.2 ± 0.2	1.07 ± 0.05	3.33 ± 0.09
		75.2	1.97± 0.08	10.3 ± 0.5	2.68 ± 0.03	10.7 ± 0.4
VR	35.6	57.7	1.02 ± 0.07	3.3 ± 0.3	0.98 ± 0.08	3.6 ± 0.1
		75.2	2.7 ± 0.1	5.8 ± 0.4	3.1 ± 0.3	11.1 ± 0.9
Cargill	52.3	57.7	0.79 ± 0.04	2.9 ± 0.1	0.78 ± 0.06	3.0 ± 0.2
		75.2	2.8 ± 0.2	6.1 ± 0.5	2.86 ± 0.04	8.0 ± 0.3
VR	52.3	57.7	1.06 ± 0.07	3.4 ± 0.2	1.04 ± 0.08	3.1 ± 0.2
		75.2	3.4 ± 0.1	7.2 ± 0.3	3.7 ± 0.3	10.2 ± 1

733 [a] Mean and standard deviation (n >21) are shown.
734 [b] k_T is the total rate constant of AA oxidation (eq. 2).

735

736

737

738

*Graphical Abstract (for review)

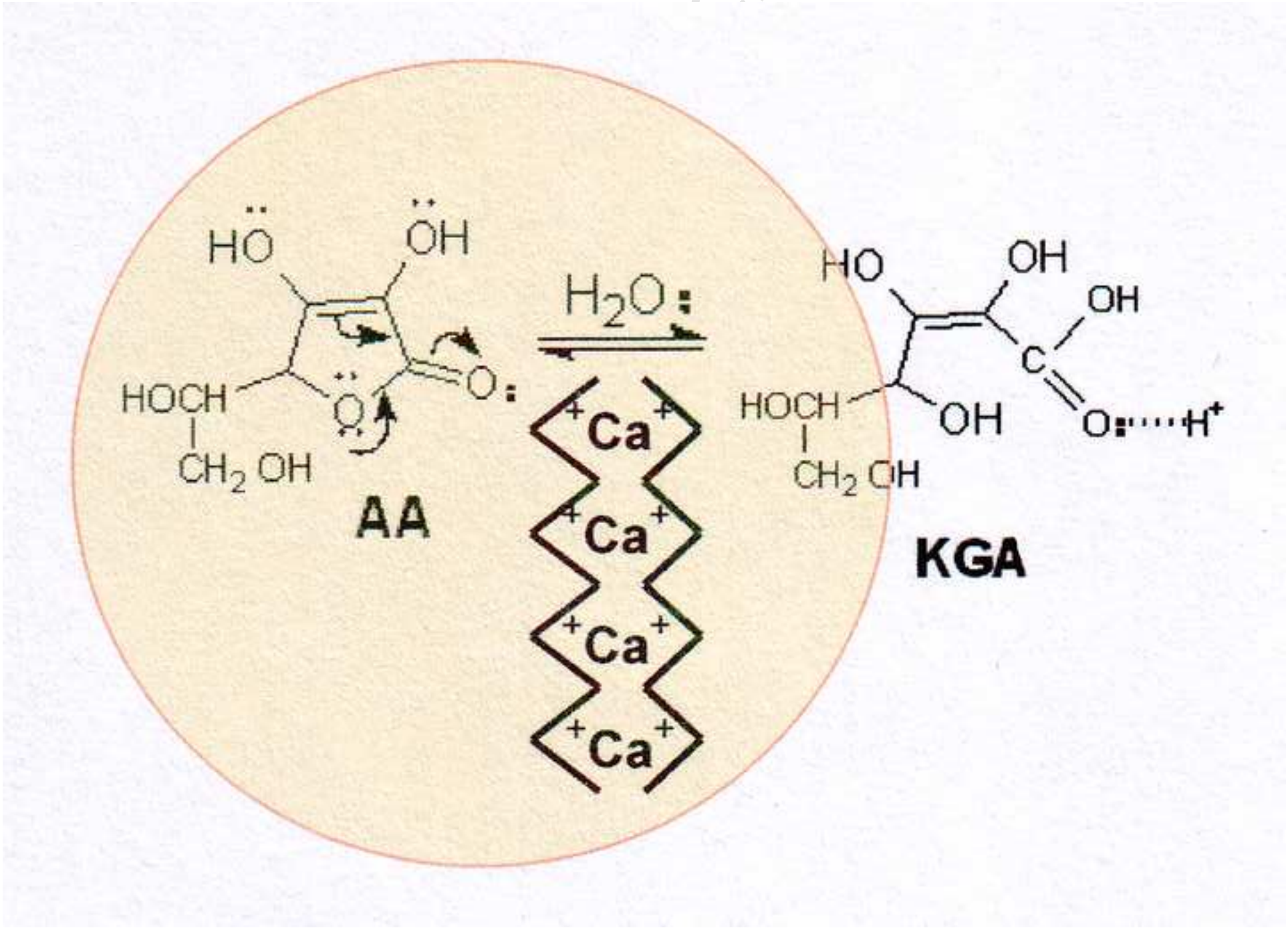

Figure(s)

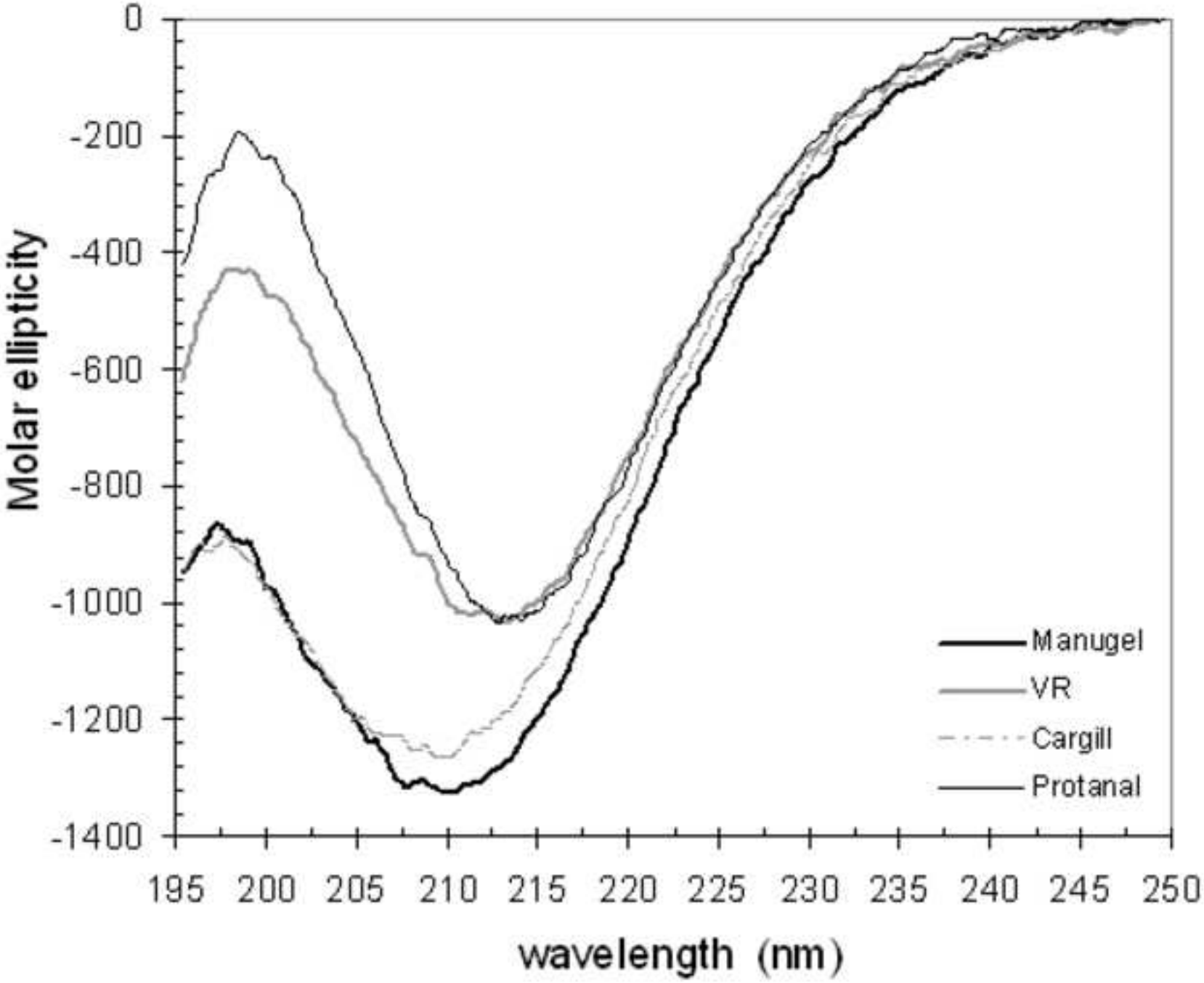
0
-200
-400
-600
-800
-1000
-1200
-1400
Molar ellipticity
195
200
205
210
215
220
225
230
235
240
245
250
wavelength (nm)
Manugel
VR
Cargill
Protanal

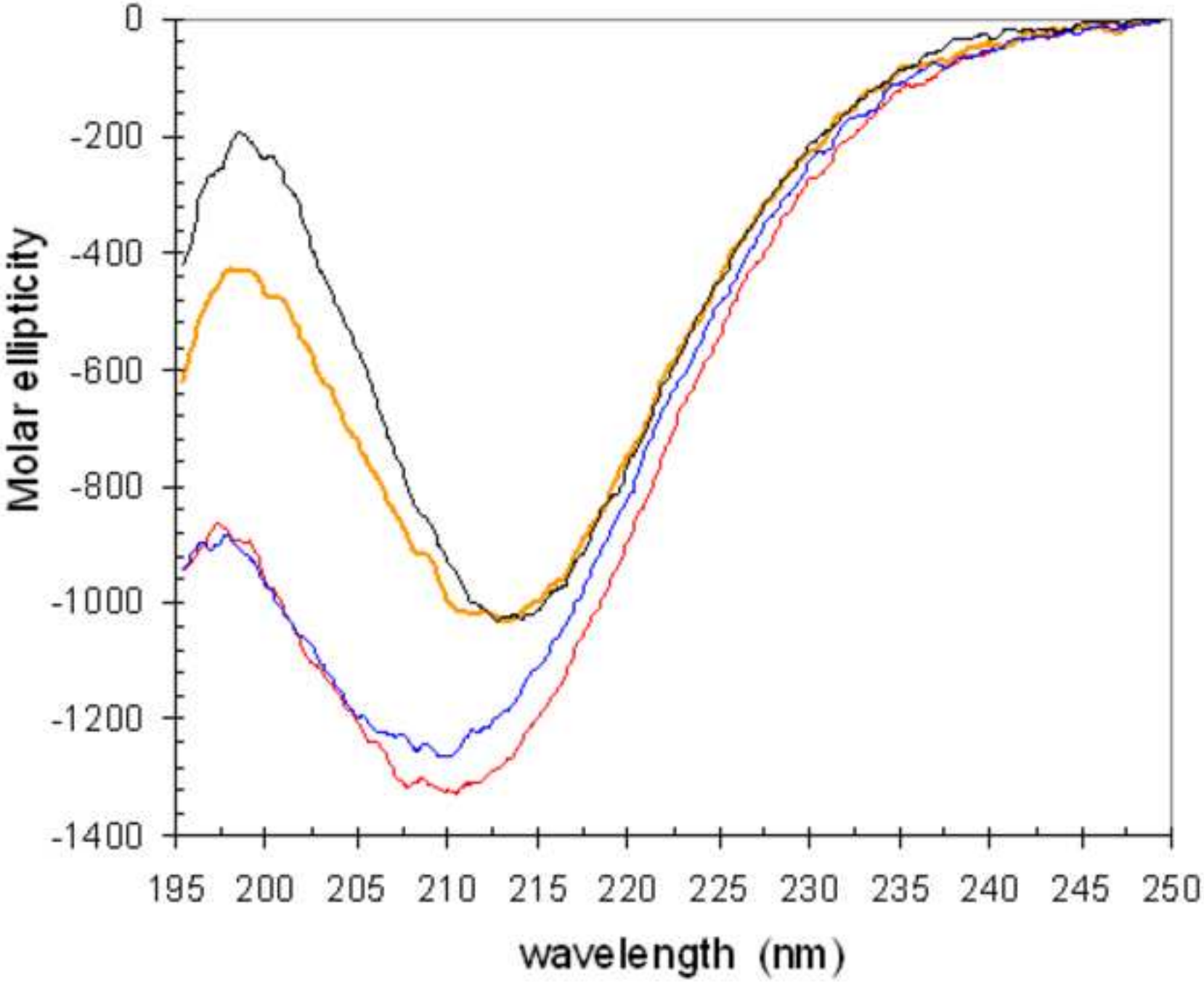
0
-200
-400
-600
-800
-1000
-1200
-1400
Molar ellipticity
195
200
205
210
215
220
225
230
235
240
245
250
wavelength (nm)

Fig. 2

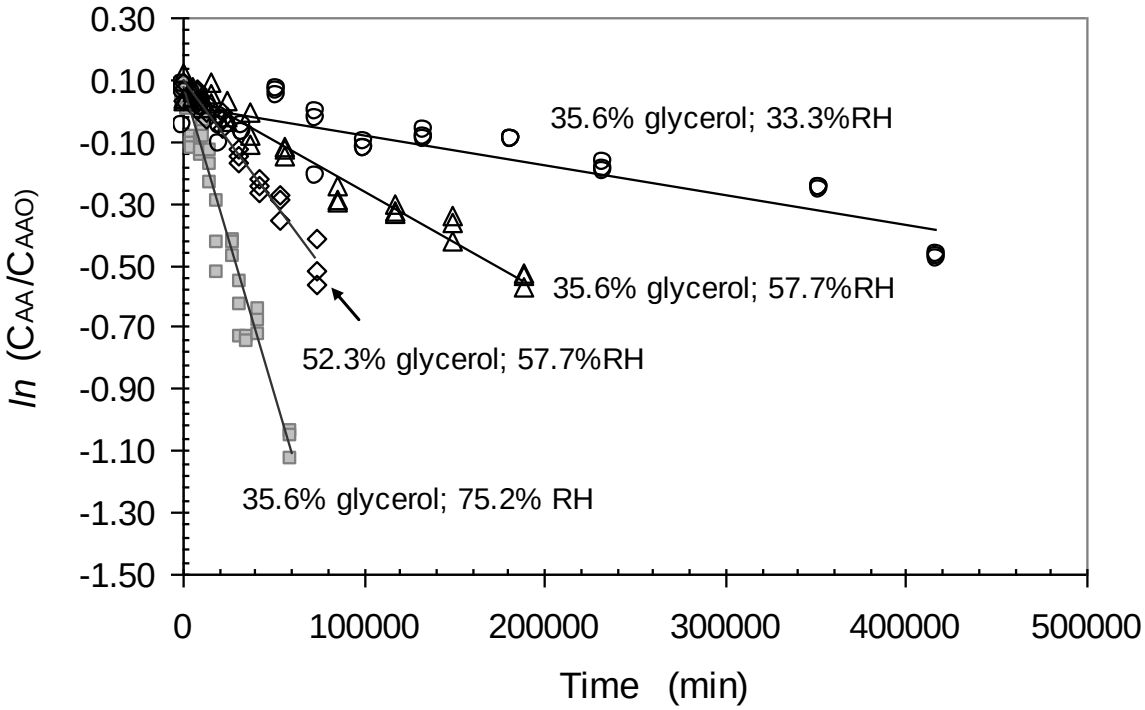

Fig. 4

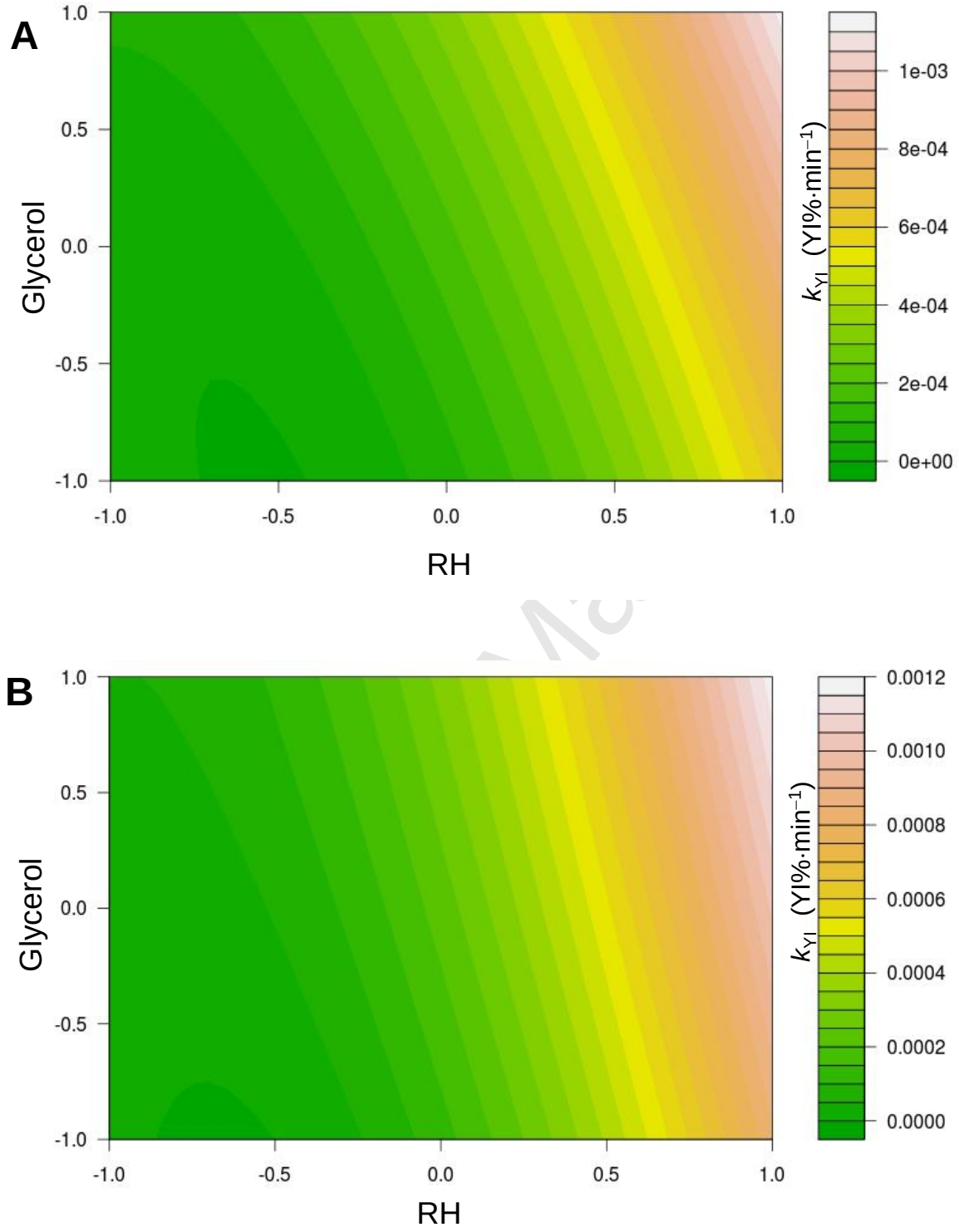

Figure(s)

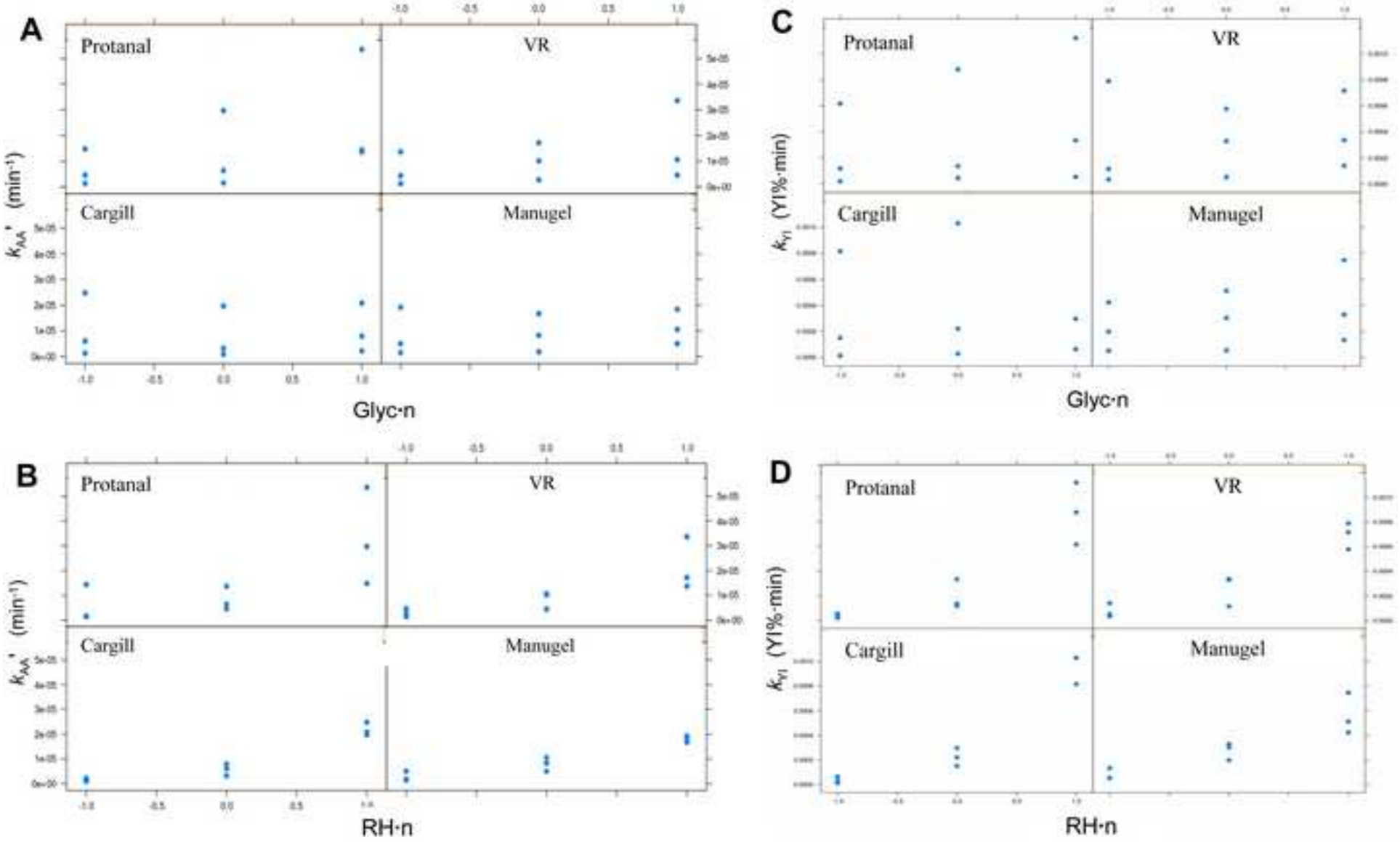
A
Protanal
VR
Cargill
Manugel
k_{AA}' (min^{-1})
Glyc·n
B
Protanal
VR
Cargill
Manugel
k_{AA}' (min^{-1})
RH·n
C
Protanal
VR
Cargill
Manugel
k_{YI} (YI%·min)
Glyc·n
D
Protanal
VR
Cargill
Manugel
k_{YI} (YI%·min)
RH·n